Journal of Materials Chemistry A

Performance Improvement of Air Electrode for Li/Air Batteries by Hydrophobicity Adjustment

Mei Chen [a, b], Jiang Xiaoliang [c], Hui Yang [d], Pei Kang Shen [a,*]

[a] *Advanced Energy Materials Research Laboratory, School of Physics and Engineering, Sun Yat-sen University, Guangzhou, 510275, China*
[b] *Dongfeng Nissian Passenger Vehicle Company, Guangzhou 510800，China*
[c] *Jiangmen Entry-Exit Inspection and Quarantine Bureau，Jiangmen 529000，China*
[d] *The Shanghai Advanced Research Institute, Shanghai 200050, China*
*Corresponding author. *E-mails:* stsspk@mail.sysu.edu.cn

Abstract: In this paper, a particular air electrode structure for Li/air batteries was designed and evaluated by using carbon paper as the support of catalyst and the current collector of the air electrode. It was demonstrated that waterproof treatment of the carbon paper with poly tetra fluoro ethylene (PTFE) enhanced its hydrophobicity, which is beneficial to the inward gas diffusion, prevention of moisture permeation and hold of the electrolyte at the same time. The Li/air battery using waterproof carbon paper with 30% PTFE and nonmetal catalyst presents a maximum specific capacity of 2367.6 mAh g^{-1} at the discharge current density of 0.1 mA cm^{-2}. Additionally, the discharge stability is quite good.

Keywords: carbon paper; waterproof treatment; hydrophobicity; air electrode; Li/air batteries

1. Introduction

Recently, the research and development of various electric, hybrid electric and plug-in hybrid electric vehicles (EV, HEV, and PHEV) for automobiles have captured increasing international concern [1-3]. The major technical hurdle for the vehicle electrification is the insufficient storage capacity of current batteries. The challenge of searching for a battery system with an energy density beyond traditional Li-ion batteries promotes the research of Li/air batteries. In a Li/air battery system, the cathode material, oxygen, can be absorbed directly from the ambient environment during the discharge process [4-6]. Among all practical electrochemical couples, Li/air has the largest theoretical specific energy of 11972 Wh kg^{-1} [7].

Since Abraham and Jiang [8] first reported Li/air batteries with non-aqueous electrolyte, extensive efforts have been made to improve the performance of Li/air batteries. However, several obstacles need to be overcome for the practical application of Li/air batteries in ambient environment: e.g., sluggish oxygen diffusion and inefficient catalyst activation for oxygen reduction in non-aqueous electrolyte [9, 10] , the volatility and hydrophilic properties of common organic electrolyte [11, 12] , and the passivation of the Li metal by crossover water. A significant problem with the air electrode in Li/air batteries is that the insoluble discharge products, Li_2O and Li_2O_2, deposited on the surface of the air electrode， gradually blocked the oxygen flow pathway in the electrode and thus eventually limited the cell capacity. Therefore, lots of efforts were devoted to porous air electrode design, optimization of the pore structure [13-15] and catalyst [16-18]. A general conclusion is obtained that the mesopore volume and the porosity of the air electrode are the critical factors that affect the performance of Li/air batteries.

For ambient operation of Li/air batteries, the most urgent problem to be solved is to prevent the Li anode corrosion by moisture from environmental air. Even trace amounts of water may induce fast corrosion of the Li anode and result in poor battery performance and serious safety risks [19]. Thus, a barrier to water penetration from air should be proposed for operation in ambient atmosphere. Highly hydrophobic material is favorable for oxygen transportation but prevents water penetration, and it could improve the ambient operation life of Li/air batteries. Zhang *et al* [12] synthesized a hydrophobic ionic liquid-silica-PVDF-HFP polymer composite electrolyte and employed it as a moisture barrier. Discharge performance of Li/air battery with this hydrophobic composite electrolyte membrane in ambient atmosphere showed a high capacity of 2800 mAh g^{-1} of carbon at the discharge current density of 0.02 mA cm^{-2} in the absence of oxygen catalyst. Zhang *et al* [15] indicated that appropriate cathode structure with a good balance of hydrophobic and hydrophilic properties can develop better Li/air batteries. Muthiah *et al* [20] synthesized core-sheath nanofiber mats with superhydrophobic properties for use in Li/air batteries, but the authors did not report the performance of Li/air batteries in their paper. Zhang *et al* [19, 21] developed an O_2-selective membrane with loading hydrophobic silicone oils into porous supports such as porous metal sheets and Teflon (PTFE) films. The membrane allows oxygen to permeate through while blocking moisture. The immobilized silicone oil membrane in the porous PTFE film enabled the Li/air batteries with carbon black air electrodes to operate in ambient air (at 20% RH) for 16.3 days with a specific capacity of 789 mAh g^{-1} carbon and a specific energy of 2182Wh kg^{-1} carbon.

From the studies hereinbefore, we can see that the hydrophobicity optimization of the cathode electrode and electrolyte exhibits its significant importance for preventing lithium corrosion and electrolyte evaporation when operating in ambient atmosphere. Carbon paper has a wide application for using as the backing layer of fuel cells. In the present work, we choose carbon paper used as the current collector and the support of activated carbon material of Ketjen black EC600JD (referred to as KB hereafter), and prepare a fuel-cell analogous air-diffusion electrode. The hydrophobicity adjustment of the carbon paper is carried out by waterproof treatment with hydrophobic material of PTFE. The hydrophobicity optimization is achieved for enhancing oxygen diffusion, building barrier for moisture penetration and mitigating electrolyte evaporation.

2. Experimental

Oxygen reduction is a fundamental reaction in fuel cells and Li/air batteries [22]. In this paper, a fuel-cell analogous air-diffusion electrode was prepared applying the method of fabricating the gas diffusion layer of fuel cell. Carbon paper (TGP-H-060, E-TEK Inc. Japan) was used as the current collector and the backing layer of air electrode. Waterproof treatment procedures for the carbon paper involved dipping the carbon paper into diluted PTFE solution for several minutes, then airing and sintering at 350 ^{o}C for 0.5 hour, quantitating the treated carbon paper and repeating the abovementioned procedures to obtain final carbon paper with specified content of PTFE. Hereinafter the plain carbon paper and waterproof carbon papers with PTFE content of 10%, 20%, 30% and 40% versus the weight of plain carbon paper were labeled as CP-0, CP-10, CP-20, CP-30 and CP-40, respectively. Slurry that consisted of carbon black (KB), binder PTFE and isopropyl alcohol was mixed and dispersed by stirring and sonicating. The weight ratio of KB to PTFE was 9:1. Then, the slurry was spread layer by layer onto carbon papers with different PTFE contents. Different air electrodes can be obtained with different weight ratios of KB to PTFE, i.e. 95:5, 85:15, 80:20 and 75:25, respectively. This fabrication method for air electrode is quite simple, as KB is strongly adhesive to the carbon paper, and its loading can be controlled easily. The electrodes were then punched in the form of disks typically with a diameter of 15 mm and then dried under vacuum at 70 °C for 12 hours.

For performance test, a Swagelok cell with an air hole of 10 mm diameter placed on the cathode side to allow the oxygen flow in was assembled. Fig. 1 shows an expanded view of experimental device for Li/air battery based on carbon paper and adhesive KB as an air electrode. 1 M $LiPF_6$ in ethylene carbonate/dimethyl carbonate (1:1 v/v) solution was used as the non-aqueous electrolyte. A double-layer separator which contains a polypropylene separator (Celgard 2300) and glass fiber (Whatman GF/D microfiber filter paper) was sandwiched between a lithium metal anode and air cathode. The glass fiber could be wetted by the electrolyte very well, so it absorbed more electrolytes and compensated for the eventual loss of electrolytes in an open environment. The volume of the non-aqueous electrolyte used in each battery was about 0.15 mL. The Li/air batteries were assembled in an argon-filled glove box and evaluated by an LAND test system (Wuhan Land Electronic Co. Ltd. China) with a low voltage limit of 2.0 V in ambient conditions.

Surface morphology of the carbon paper was characterized by scanning electron microscopy (SEM) on Hitachi S-4700 microscope

The hydrophobic character of the carbon paper was evaluated by DSA100 (KRÜSS, Germany). In each measurement, a droplet water of 4 μL was placed onto the surface of the sample, and then the contact angle was immediately measured.

Photographs of top-view of the Li/air battery and the outside surfaces of the air electrode were taken using wireless digital microscope (ISM-WM200, Insize).

Electrochemical impedance spectra (EIS) were obtained using a frequency response analyzer (Solartron SI1260) coupled to a Potentiostat/Galvanostat (EG&G Model 273A). Impedance of the batteries was measured at open circuit potential in the frequency range of 100 kHz to100 mHz, with an amplitude of the sinusoidal voltage signal less than 5 mV. The resulting impedance was analyzed based on an electrical circuit element model. The Zsimpwin software was used to fit the experimental data to the equivalent circuit.

3. Results and Discussions

For air electrode, in comparing with Ni/Al mesh or foamed Ni, carbon paper is an ideal backing layer and current collector due to its light weight and high conductivity. The object of waterproof treatment of the carbon paper with PTFE is to increase its mechanical strength and hydrophobicity. Fig. 2 shows the voltage-capacity discharge curves of lithium air batteries with different carbon papers (CP-0, CP-10, CP-20, CP-30 and CP-40) in air electrode at the discharge current density of 0.1 mA cm^{-2}. The KB loading of the air electrode was about 1.6±0.1 mg cm^{-2} and the weight ratio of KB to PTFE in the slurry of the batteries with different carbon paper here is the same, 9:1. From Fig. 2, the initial discharging voltage increases with the increase in PTFE content. Discharging to 2.0 V, the specific capacity (mAh g^{-1} carbon) for each cell has the following order from high to low: CP-30>CP-20≈CP-40>CP-10>CP-0. For the carbon paper without waterproof treatment (CP-0), the electrolyte can permeate outward easily and the battery can not discharge stably. The discharging voltage drops gradually and its specific capacity is only 1361.2 mAh g^{-1}. After waterproof treatment by PTFE, there was a stable voltage section on each discharging curve. The maximum specific capacity of 2367.6 mAh g^{-1} was reached for CP-30.

Discharge-charge profiles for 5 cycles of the lithium/air battery with CP-0 and CP-30 at 0.1 mA cm^{-2} was investigated. The voltage profiles of the 1 st, 2 nd, and 5 th cycles are shown in Fig. 3. It was observed that the discharge capacities of the lithium/air battery with CP-0 at the 1st, 2 nd, and 5 th cycle were 1361.2, 474.0 and 69.5 mAh g^{-1}, respectively. And the discharge capacities of CP-30 were 2367.6, 974.4 and 320.4 mAh g^{-1}, respectively. The lithium/air battery with CP-30 exhibits better discharge performance than that with CP-0 obviously. The charge behavior of the battery with CP-30 possesses improved performance. Thus, the discharge-charge profiles indicate that the hydrophobicity optimization promote the initial discharge capacity and the cycle performance.

Fig. 4 presents the discharge behavior of the lithium air battery with CP-0 and CP-30 at rates of 0.05, 0.2 and 0.5 mA cm^{-2}. The cell of CP-30 delivers a huge capacity of 2706.9 mAh g^{-1} of carbon at a relatively low current density of 0.05 mA cm^{-2}. However, the specific capacity and operating voltage drop significantly with increasing discharge current density [2, 23]. The discharge capacity of the cell decreases to 1611.7 mAh g^{-1}at a current density of 0.2 mA cm^{-2}, and only 326.3 mAh g^{-1} was obtained at 0.5 mA cm^{-2}. The battery of CP-0 had similar rate performance. But its degradation of rate capability is more seriously. Read *et al* [2] found that all of the pores in air electrode were filled which ends discharge at low rate and a film formed on the air side of the electrode discharged at high current density appears to limit discharge in the interior of the electrode.

Fig.5 shows the plots of capacity or specific capacity versus carbon loading for the battery with CP-30 at the constant current density of 0.1mA cm^{-2}. The capacity increases but the specific capacity decreases as carbon loading is increased. This behavior has been reported by other groups [5, 24] and it is emphasized that adequate oxygen diffusion is important to achieve high gravimetric capacity [25].

In order to clarify the influence of the hydrophobicity of carbon paper on cell performance, SEM, the contact angle and EIS measurements were conducted. Fig. 6 presents the SEM micrographs of various carbon papers and air electrodes. Fig. 6(A) and (B) are for CP-0 and CP-30, respectively. Fig. 6(C) and (D) are for the air electrode in which KB catalyst is spread on carbon paper with different magnifications. Fig. 6(E) is the air electrode after discharge. From Fig. 6(A) and (B), it can be seen that there is uniform continuous carbon fiber network on both CP-0 and CP-30, which favors gas transportation uniformly and improves the discharge stability. And a PTFE membrane exists on the carbon fiber surface of CP-30. After coated with KB, the macropores on carbon fiber were filled as shown in Fig. 6(C). The KB was distributed homogeneously on the surface of the carbon paper and abundant smaller pores were formed under the accumulation of KB as shown in Fig. 6(D). Fig. 6(E) shows that the discharge products were deposited and grown up on the surface of KB. They can cover the oxygen reduction active sites, block the gas flow pathway, and eventually limit the cell capacity.

The hydrophobicity of the carbon paper could be characterized by angle contact measurement. Fig. 7 compares the contact angle of water droplet placed on CP-0 and CP-30. As indicated in Fig. 7(A), a contact angle of 136.6^{o} was observed when water droplet is on CP-0. After treated with PTFE, a waterproof membrane formed as shown in Fig. 7(B) and the contact angle for CP-30 increased to 148.3^{o}. The PTFE treatment of carbon paper results in more hydrophobic on the surface of the pores accumulated by PTFE coated carbon fiber. The surface hydrophobicity can prevent water vapor condensation from ambient air and its subsequent penetration into the membrane [19]. The hydrophobic carbon paper establishes selective permeation of O_2 over H_2O.

At the same time, the increased hydrophobicity would also be beneficial to hold the electrolyte and minimize the solvent loss from the battery into ambient air due to evaporation. Fig.8 shows photographs of air electrode of the Li/air batteries with CP-0 and CP-30. The two batteries seem to be similar from top-view as shown in Fig.8 (A). On Fig.8 (B), the air electrode with CP-0 is flooded by electrolyte. There is electrolyte overflow on the surface of CP-0, especially at the edge of the air hole. The evaporation of overflowed electrolyte is suggested to attribute to the instability during discharge. In a flooded air electrode, the oxygen has to dissolve into the electrolyte at the carbon paper–oxygen interface and the kinetics of this system is slow because oxygen in solution is less mobile than that in the gaseous phase. Fig.8 (C) indicates no overflowed electrolyte exists on the carbon paper outside the battery with CP-30. The electrolyte is held in the electrode and a wetted air electrode is formed. It maintains the oxygen diffusion length through the cathode which increases the oxygen kinetics and creates a more uniform concentration of oxygen and lithium ions in the cathode [26].

To further study the effect of carbon paper's hydrophobicity on its electrochemical performance, the impedance behavior of Li/air batteries with CP-0 and CP-30 before and after discharge was comparatively investigated. Fig. 9 shows the experimental Nyquist plot of the batteries and results of data simulation based on an equivalent circuit shown in inset. R_e represents the bulk ohmic resistance. R_{ct} denotes the charge-transfer resistance. R_{int} is the interfacial resistance between electrode and electrolyte. Two constant phase elements, Q_1 and Q_2, correspond to the associated capacitance. W is the Warburg diffusion contribution.

Fig. 9 shows that the simulated curve fits entirely with the data measured over the full range of frequencies, indicating that the proposed equivalent circuit represents the cell impedance well. The parameters obtained from the fitting are given in Table 1. The ohmic resistance R_e, corresponding to the intercept in the high-frequency domain on the Z' axis, is larger for the battery with CP-30 than the battery with CP-0 before discharge. In the former case the carbon paper is treated by PTFE for waterproofing and this polymer is an insulator. The higher PTFE content and increased hydrophobicity lead to lower conductivity and less contact at interface, giving rise to a larger interfacial contact resistance (R_{int}) at the same time. However, the battery with CP-30 possesses a lower charge-transfer resistance R_{ct} (119.9 ohm) than that with CP-0 (135.2 ohm). During discharge, large amounts of poor electronic conductive precipitates, Li_2O_2 and Li_2O, are generated, and the chocked air electrode results in a dramatic increase in resistance. After discharge, the charge-transfer resistance rises obviously. Moreover, the charge-transfer resistance increase for CP-0 (from 135.2 to 482.2 ohm) is significantly larger than that for CP-30 (from 119.9 to 287.3 ohm). This phenomenon suggests that high hydrophobicity carbon paper is needed to sustain long and stable discharging.

The hydrophobicity optimization in the nonmetal catalyst layer of the air electrode was further investigated. For preparing a uniform catalyst layer with different hydrophobicities, slurries with KB and different PTFE contents were loaded on the CP-30. The PTFE content in the catalyst was expected to relate with the porosity and hydrophobicity of the air electrode. The KB loading of the air electrode was about 1.6±0.1 mg cm^{-2}. Fig. 10 shows the voltage-discharge capacity profiles for Li/air batteries with different PTFE contents in the catalyst layer at the discharge current density of 0.1 mA cm^{-2}. It can be seen that all the discharge curves are flat and the PTFE content in the catalyst layer has a significant effect on the cell specific capacity. The maximum specific capacity achieved 3107.7 mAh g^{-1} when the PTFE content was 20%.

4. Conclusions

A new type of air electrode for Li/air batteries was designed and optimized by using carbon paper as the backing layer of the active material and the current collector of the electrode. Waterproof treatment of carbon paper and adjustment of the PTFE content in carbon catalyst both favor the performance improvement of the battery. The results of SEM, the contact angle measurement and photograph of the external surface of the air electrode suggested that waterproof treatment of carbon paper is beneficial for pore modification, high hydrophobicity and electrolyte holding, thus improves capacity and discharge stability of Li/air batteries. PTFE content of the catalyst layer in air electrode also affects the hydrophobicity and its optimized value is 20 %.

References:

[1] G. Girishkumar, B. McCloskey, A. C. Luntz, S. Swanson,W. Wilcke, The Journal of Physical Chemistry Letters 1(2010) 2193-2203.

[2] C. Tran, X. Yang,D. Qu, J. Power Sources 195(2010) 2057-2063.

[3] P. G. Bruce, S. A. Freunberger, L. J. Hardwick,J. Tarascon, Nature Materials 11(2012) 19-29.

[4] J. Read, J. Electrochem. Soc. 149(2002) A1190-A1195.

[5] S. D. Beattie, D. M. Manolescu,S. L. Blair, J. Electrochem. Soc. 156(2009) A44-A47.

[6] R. E. Williford,J. Zhang, J. Power Sources 194(2009) 1164-1170.

[7] T. Ogasawara, A. Débart, M. Holzapfel, P. Novák,P. G. Bruce, J. Am. Chem. Soc. 128(2006) 1390-1393.

[8] K. M. Abraham,Z. Jiang, J. Electrochem. Soc. 143(1996) 1-5.

[9] C. O. Laoire, S. Mukerjee, K. M. Abraham, E. J. Plichta,M. A. Hendrickson, The Journal of Physical Chemistry C 113(2009) 20127-20134.

[10] J. Zhang, D. Wang, W. Xu, J. Xiao,R. E. Williford, J. Power Sources 195(2010) 4332-4337.

[11] W. Xu, J. Xiao, J. Zhang, D. Wang,J. Zhang, J. Electrochem. Soc. 156(2009) A773-A779.

[12] D. Zhang, R. Li, T. Huang,A. Yu, J. Power Sources 195(2010) 1202-1206.

[13] X. H. Yang, P. He,Y. Y. Xia, Electrochem. Commun. 11(2009) 1127-1130.

[14] M. Mirzaeian,P. J. Hall, J. Power Sources 195(2010) 6817-6824.

[15] T. Zhang, N. Imanishi, Y. Shimonishi, A. Hirano, Y. Takeda, O. Yamamoto,N. Sammes, Chem. Commun. 46(2010) 1661-1663.

[16] A. Débart, A. J. Paterson, J. Bao,P. G. Bruce, Angewandte Chemie International Edition 47(2008) 4521-4524.

[17] H. Cheng,K. Scott, Applied Catalysis B: Environmental In Press, Accepted Manuscript(

[18] Y. Wang,H. Zhou, Chem. Commun. 46(2010) 6305-6307.

[19] J. Zhang, W. Xu, X. Li,W. Liu, J. Electrochem. Soc. 157(2010) A940-A946.

[20] P. Muthiah, S. Hsu,W. Sigmund, Langmuir 26(2010) 12483-12487.

[21] J. Zhang, W. Xu,W. Liu, J. Power Sources 195(2010) 7438-7444.

[22] B. Kumar,J. Kumar, J. Electrochem. Soc. 157(2010) A611-A616.

[23] D. Zhang, Z. Fu, Z. Wei, T. Huang,A. Yu, J. Electrochem. Soc. 157(2010) A362-A365.

[24] J. Xiao, D. Wang, W. Xu, D. Wang, R. E. Williford, J. Liu,J. Zhang, J. Electrochem. Soc. 157(2010) A487-A492.

[25] J. Read, J. Electrochem. Soc. 149(2002) A1190-A1195.

[26] S. S. Sandhu, J. P. Fellner,G. W. Brutchen, J. Power Sources 164(2007) 365-371.

Figure captions

Fig. 1 Schematic representation of the lithium/air battery in exploded view.

Fig. 2 Discharge curves of lithium/air batteries with different hydrophobic carbon paper in air electrode in ambient atmosphere at the discharge current density of 0.1 mA cm^{-2}.

Fig.3 Discharge-charge profiles of the 1st, 2nd, and 5th cycles for the lithium/air battery with CP-0 and CP-30 at 0.1mA cm^{-2}

Fig. 4 Discharge curves of lithium/air battery with (a) CP-0 and (b) CP-30 at different rates.Fig. 5 Capacity and specific capacity versus carbon loading for the lithium/air battery with CP-30 at 0.1mA cm^{-2}.

Fig. 6 SEM micrographs of (A) CP-0, (B) CP-30, (C) and (D) air electrode, (E) air electrode after discharging.

Fig. 7 The contact angles of water distributed on two different hydrophobic carbon paper. (A) carbon paper with no wet proofing and (B) carbon paper with 30% wet proofing.

Fig.8 Photographs of top-view of the Li/air batteries (A), the outside surfaces of the air electrode with CP-0 (B) and CP-30 (C).

Fig. 9 Impedance spectra of lithium/air batteries with different hydrophobic carbon paper in air electrode before and after discharging

Fig. 10 Discharge curves of lithium/air batteries with different PTFE content in KB slurry in ambient atmosphere at the discharge current density of 0.1mA cm^{-2}.

Table 1 Fitted parameters for the CPE-based equivalent circuit model for the two lithium/air batteries with different hydrophobicity carbon paper in air electrode before and after discharging.

Parameter	CP-0	CP-30	CP-0 after discharge	CP-30 after discharge
R_e/ ohm	13.5	22.0	215.7	53.7
R_{int}/ ohm	141.1	272.6	272.1	168.6
Q_1 / F	0.003	0.001	0.001	0.005
n_1	0.8	0.5	0.8	0.8
R_{ct}/ ohm	135.2	119.9	468.2	287.3
Q_2 / F	4.9E-5	8.1E-5	1.4E-5	4.9E-5
n_2	0.6	0.8	0.6	0.8
W / ohm	0.006	0.005	0.004	0.004

Fig. 1


Lithium metal
Separator
Glass fiber
Carbon catalyst
Carbon paper

Fig. 2

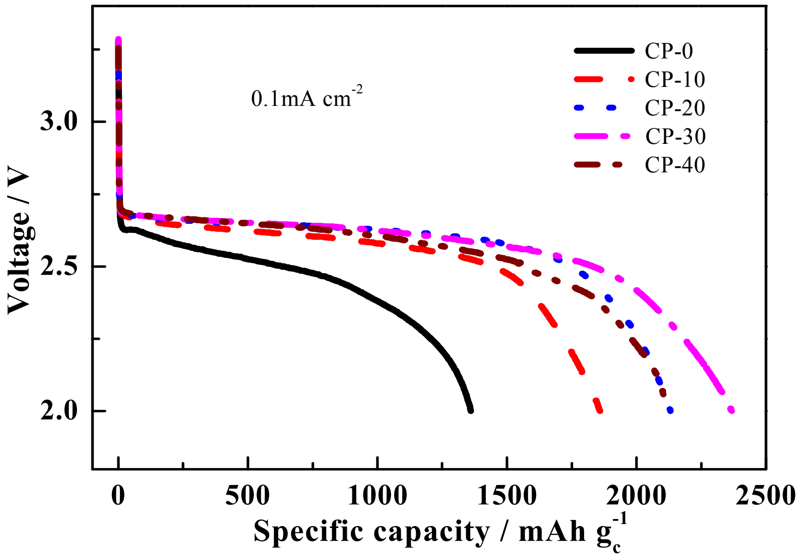

CP-0
CP-10
CP-20
CP-30
CP-40
0.1mA cm^{-2}
Voltage / V
3.0
2.5
2.0
0
500
1000
1500
2000
2500
Specific capacity / mAh g_c^{-1}

Fig. 3

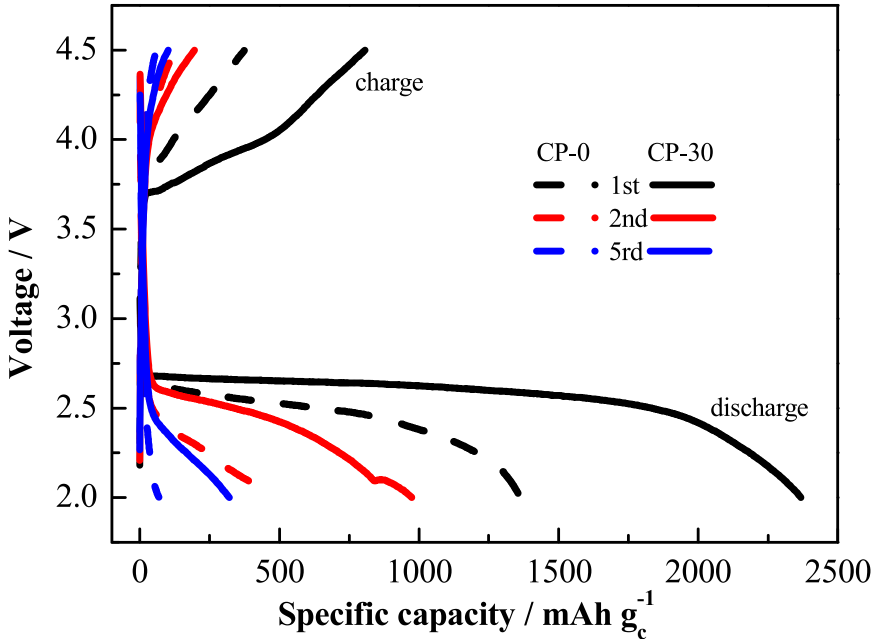
4.5
4.0
3.5
3.0
2.5
2.0
Voltage / V
0
500
1000
1500
2000
2500
Specific capacity / mAh g_c^{-1}
charge
discharge
CP-0
CP-30
1st
2nd
5rd

Fig. 4

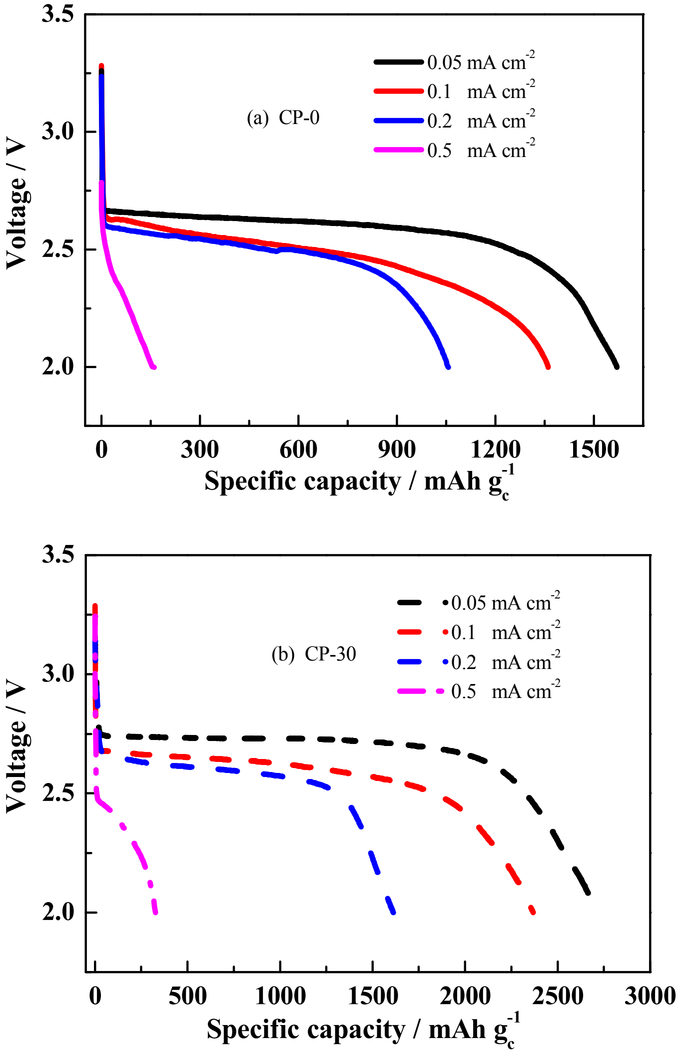
(a) CP-0
0.05 mA cm^{-2}
0.1 mA cm^{-2}
0.2 mA cm^{-2}
0.5 mA cm^{-2}
Voltage / V
3.5
3.0
2.5
2.0
0
300
600
900
1200
1500
Specific capacity / mAh g$_c^{-1}$
(b) CP-30
0.05 mA cm^{-2}
0.1 mA cm^{-2}
0.2 mA cm^{-2}
0.5 mA cm^{-2}
Voltage / V
3.5
3.0
2.5
2.0
0
500
1000
1500
2000
2500
3000
Specific capacity / mAh g$_c^{-1}$

Fig. 5

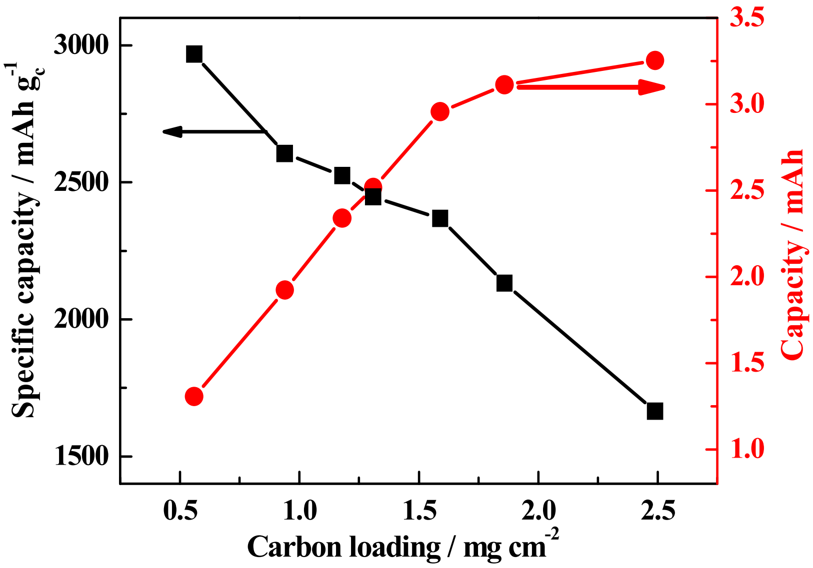
Specific capacity / mAh g_c^{-1}
3000
2500
2000
1500
Capacity / mAh
3.5
3.0
2.5
2.0
1.5
1.0
0.5
1.0
1.5
2.0
2.5
Carbon loading / mg cm^{-2}

Fig. 6

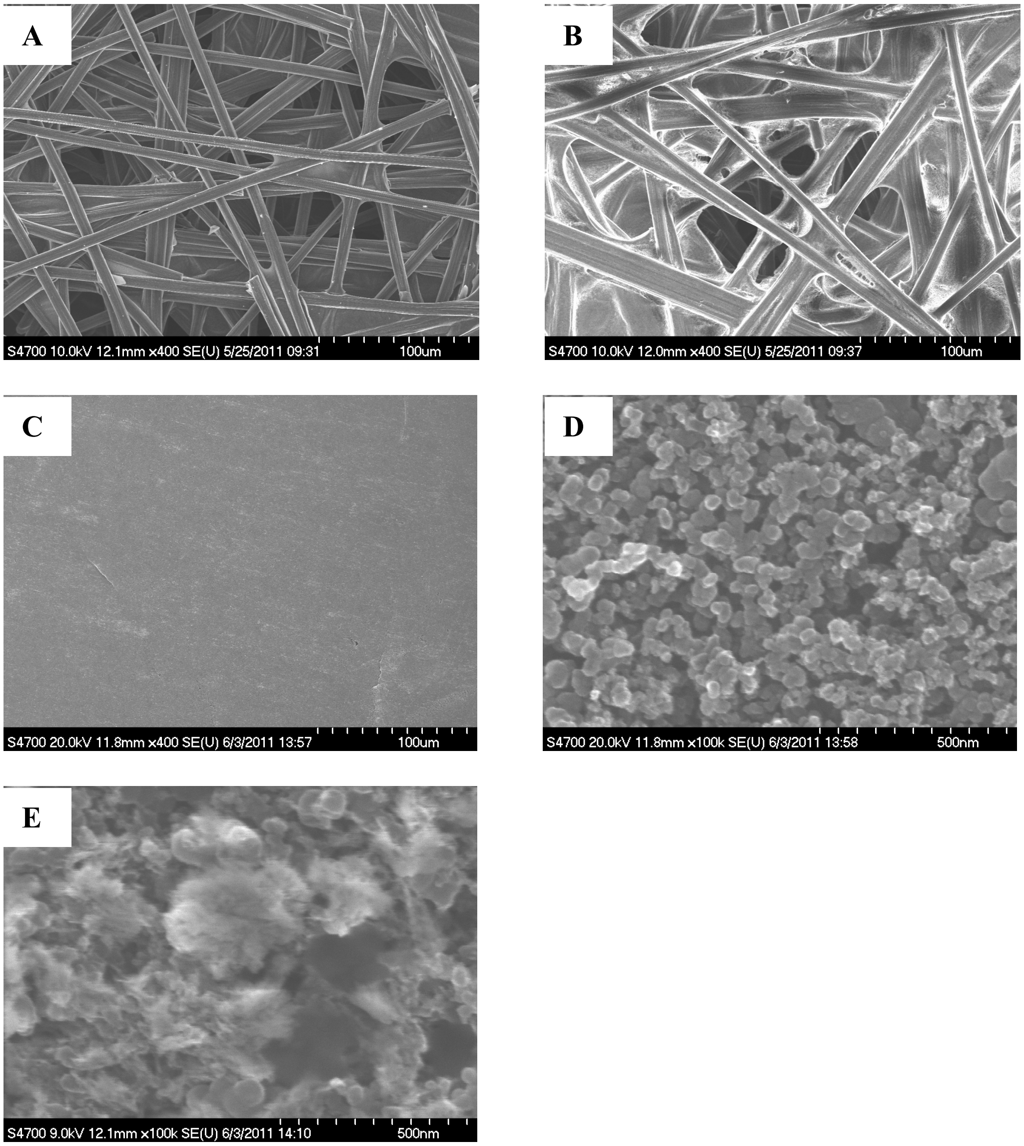
A
S4700 10.0kV 12.1mm x400 SE(U) 5/25/2011 09:31 100um
B
S4700 10.0kV 12.0mm x400 SE(U) 5/25/2011 09:37 100um
C
S4700 20.0kV 11.8mm x400 SE(U) 6/3/2011 13:57 100um
D
S4700 20.0kV 11.8mm x100k SE(U) 6/3/2011 13:58 500nm
E
S4700 9.0kV 12.1mm x100k SE(U) 6/3/2011 14:10 500nm

Fig.7

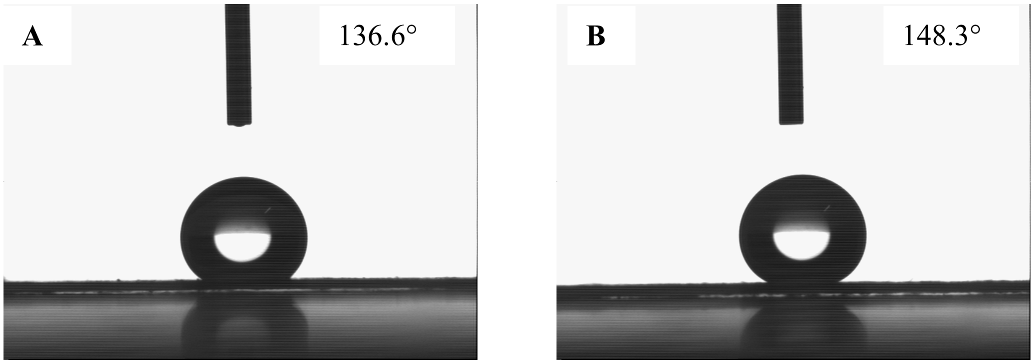

Fig. 8

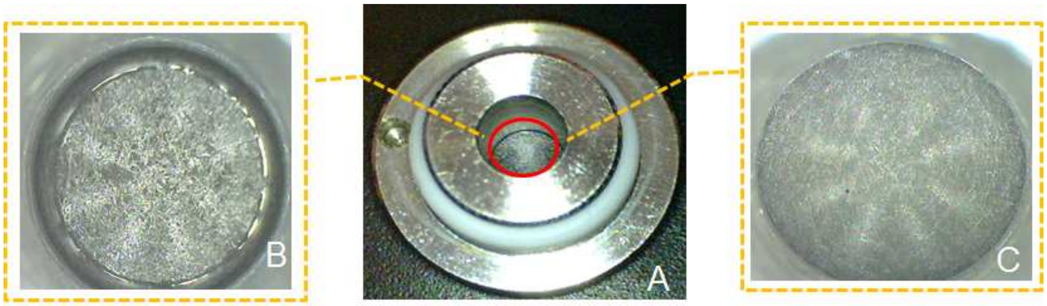

Fig. 9

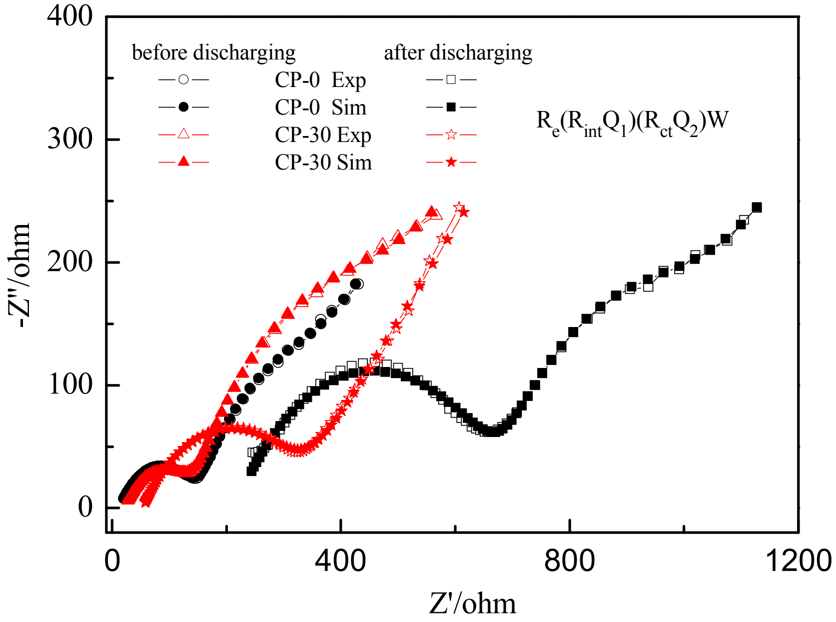
before discharging
after discharging
CP-0 Exp
CP-0 Sim
CP-30 Exp
CP-30 Sim
$R_e(R_{int}Q_1)(R_{ct}Q_2)W$
-Z''/ohm
Z'/ohm
0
100
200
300
400
0
400
800
1200

Fig. 10

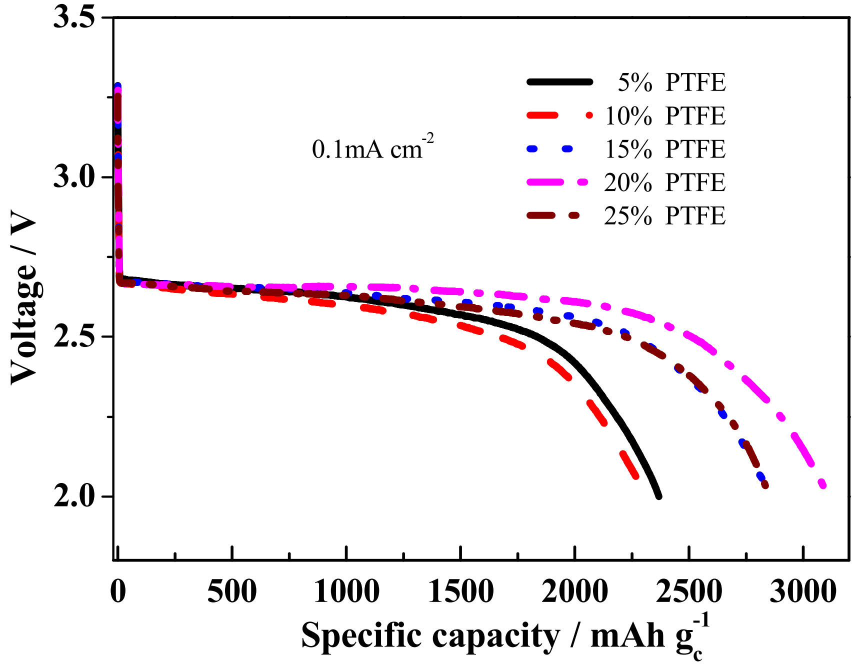

3.5
3.0
2.5
2.0
Voltage / V
0
500
1000
1500
2000
2500
3000
Specific capacity / mAh g_c^{-1}
0.1mA cm^{-2}
5% PTFE
10% PTFE
15% PTFE
20% PTFE
25% PTFE